

Complement component 3 from astrocytes mediates retinal ganglion cell loss during neuroinflammation

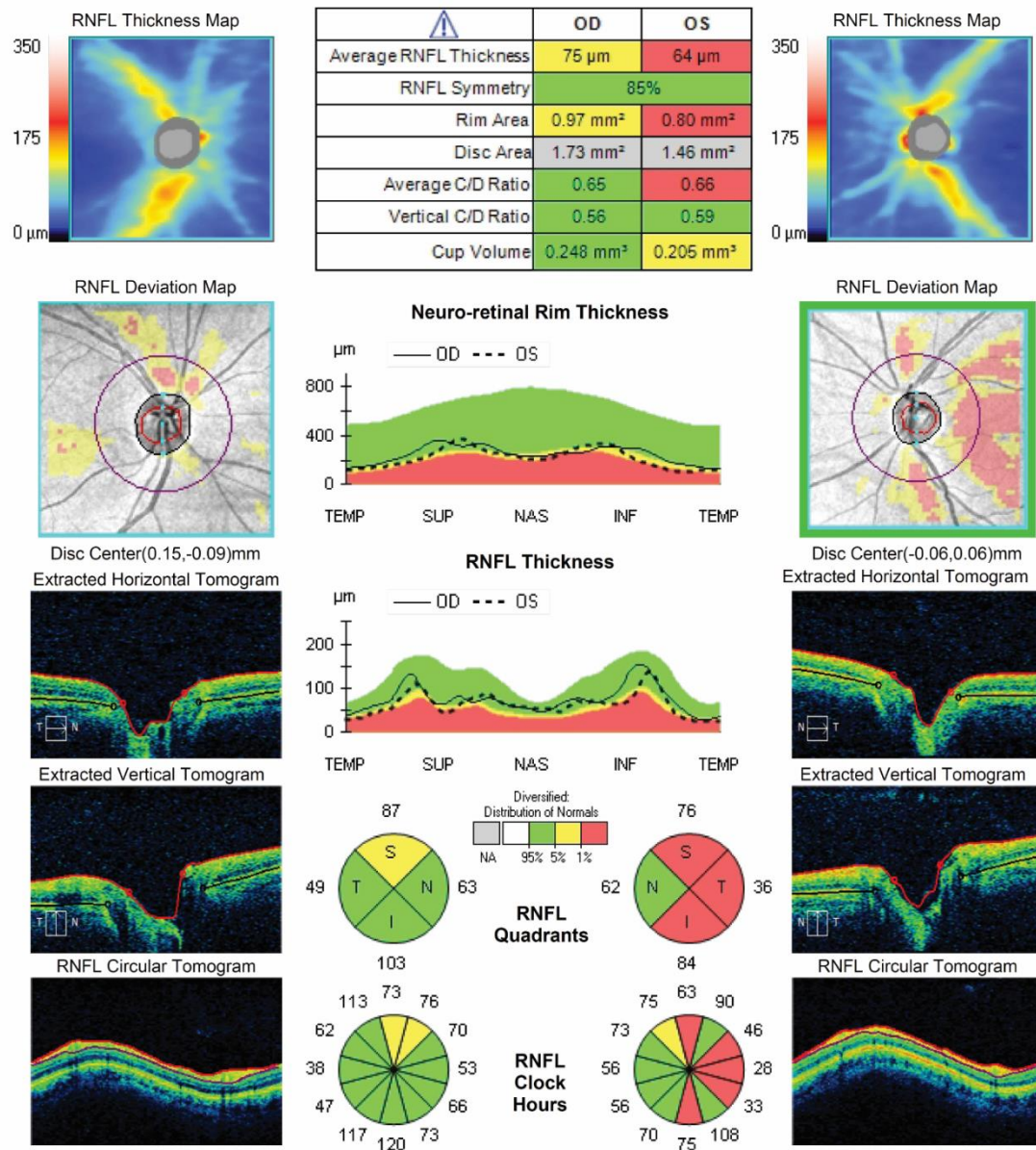
Acta Neuropathologica

Marjan Gharagozloo^{1*}, Matthew D. Smith^{1*}, Jing Jin^{1*}, Thomas Garton¹, Michelle Taylor¹, Alyssa Chao¹, Keya Meyers¹, Michael D. Kornberg¹, Donald J. Zack^{2,3,4}, Joan Ohayon⁵, Brent A. Calabresi⁵, Daniel S. Reich^{1,5}, Charles G. Eberhart^{3,6}, Carlos A. Pardo¹, Claudia Kemper^{7,8}, Katharine A. Whartenby¹, and Peter A. Calabresi^{1, 2, 3#}.

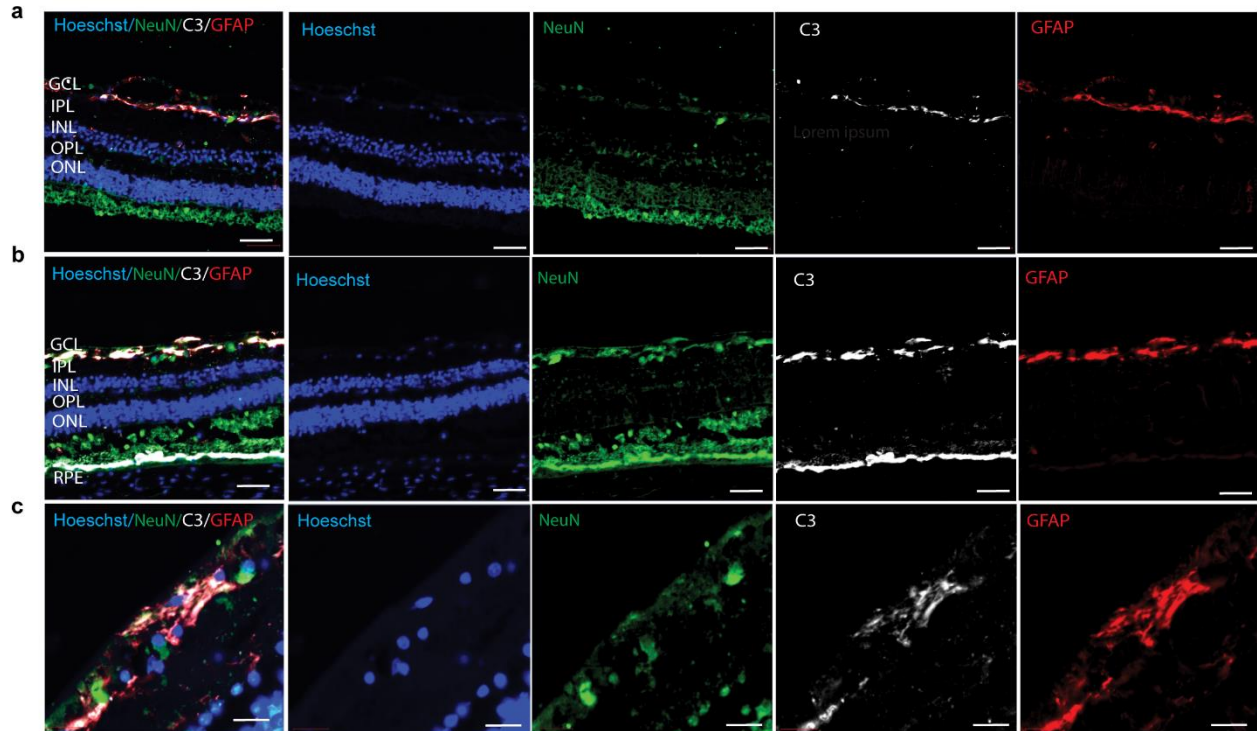
#Corresponding author: calabresi@jhmi.edu

Supplemental figures

ONH and RNFL OU Analysis: Optic Disc Cube 200x200 OD ● OS ●

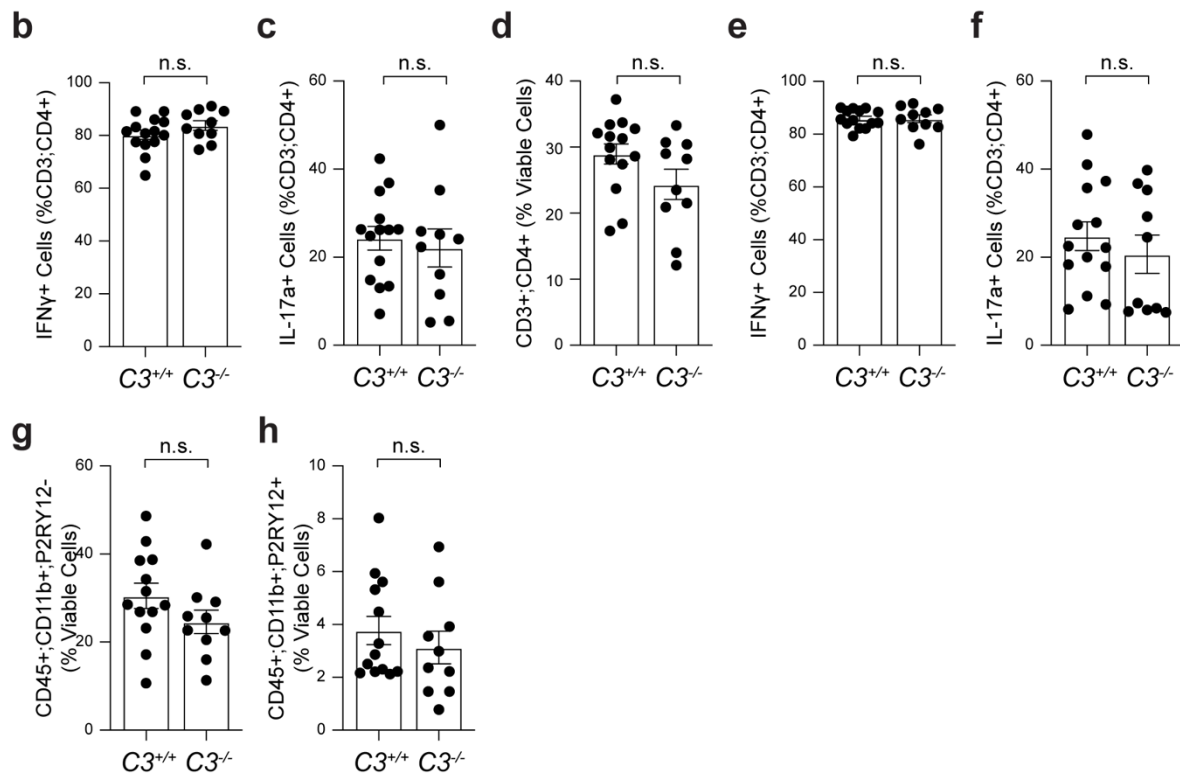
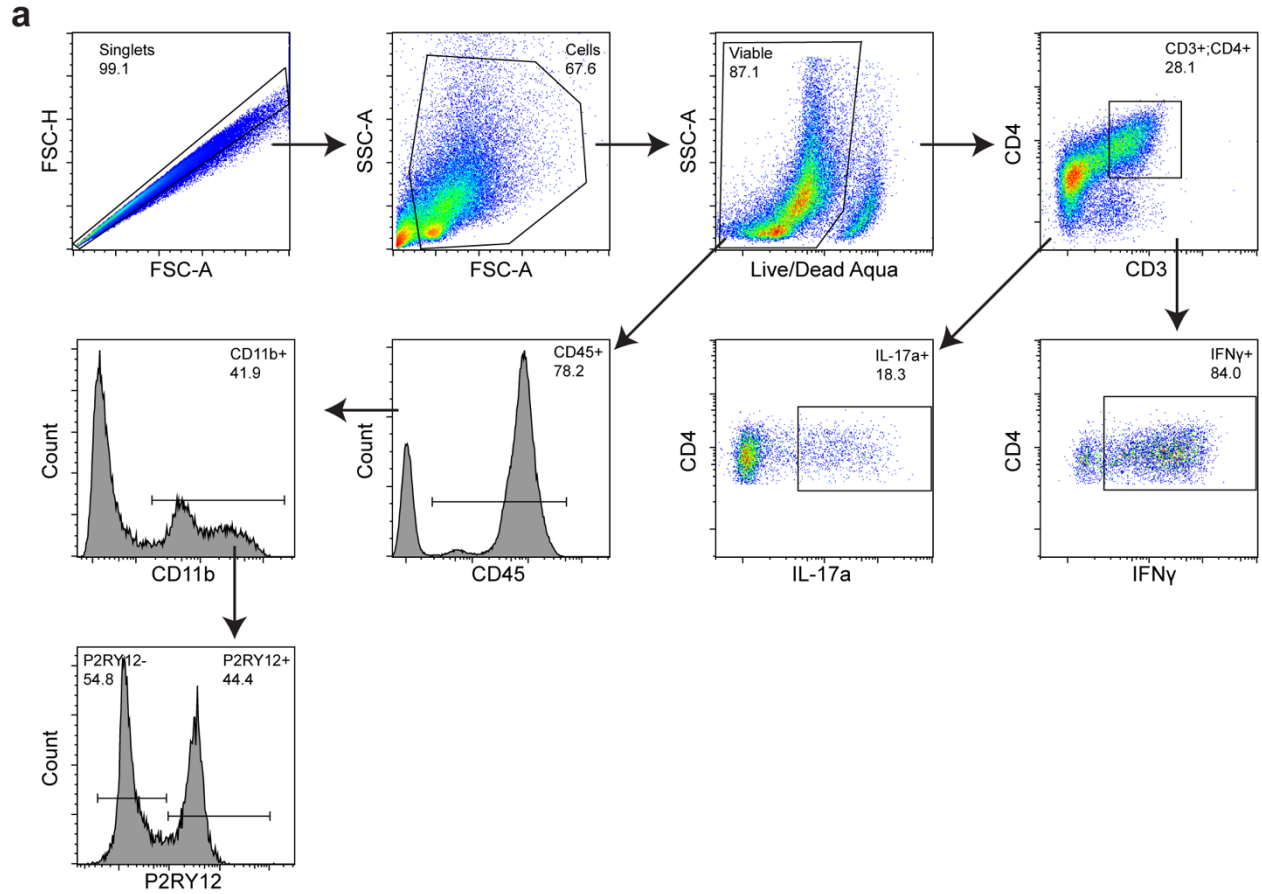


Supplementary Fig 1. Optical coherence tomography scan showing optic nerve head of the MS patient retina presented in Fig 1. Retinal nerve fiber layer (RNFL) map shows mean value OS less than 1st percentile (red) for age matched controls. RNFL mean value OD is in the 1st to 5th percentile (yellow) for age matched controls.



Supplementary Fig 2. C3 expression is heterogeneous in MS retina

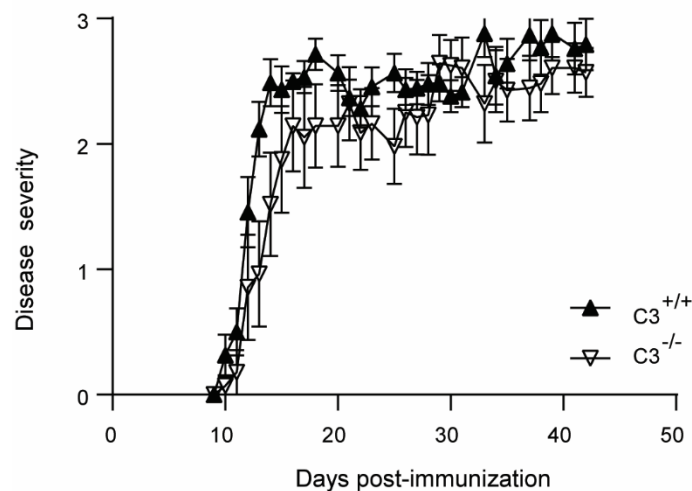
(a) Representative images of MS patient post-mortem retina with C3 expression in the ganglion cell layer (GCL); Scale bar =50 μ m. (b) Representative images of MS retina with C3 expression in GCL and retinal pigment epithelium (RPE) layer; Scale bar =50 μ m. (c) Magnified region of GCL from MS retina showing GFAP⁺ cells express C3; Scale bar =20 μ m. Each row represents C3 expression in separate individuals with MS.



Supplementary Fig 3. Global C3 depletion does not affect immune infiltrate in EAE.

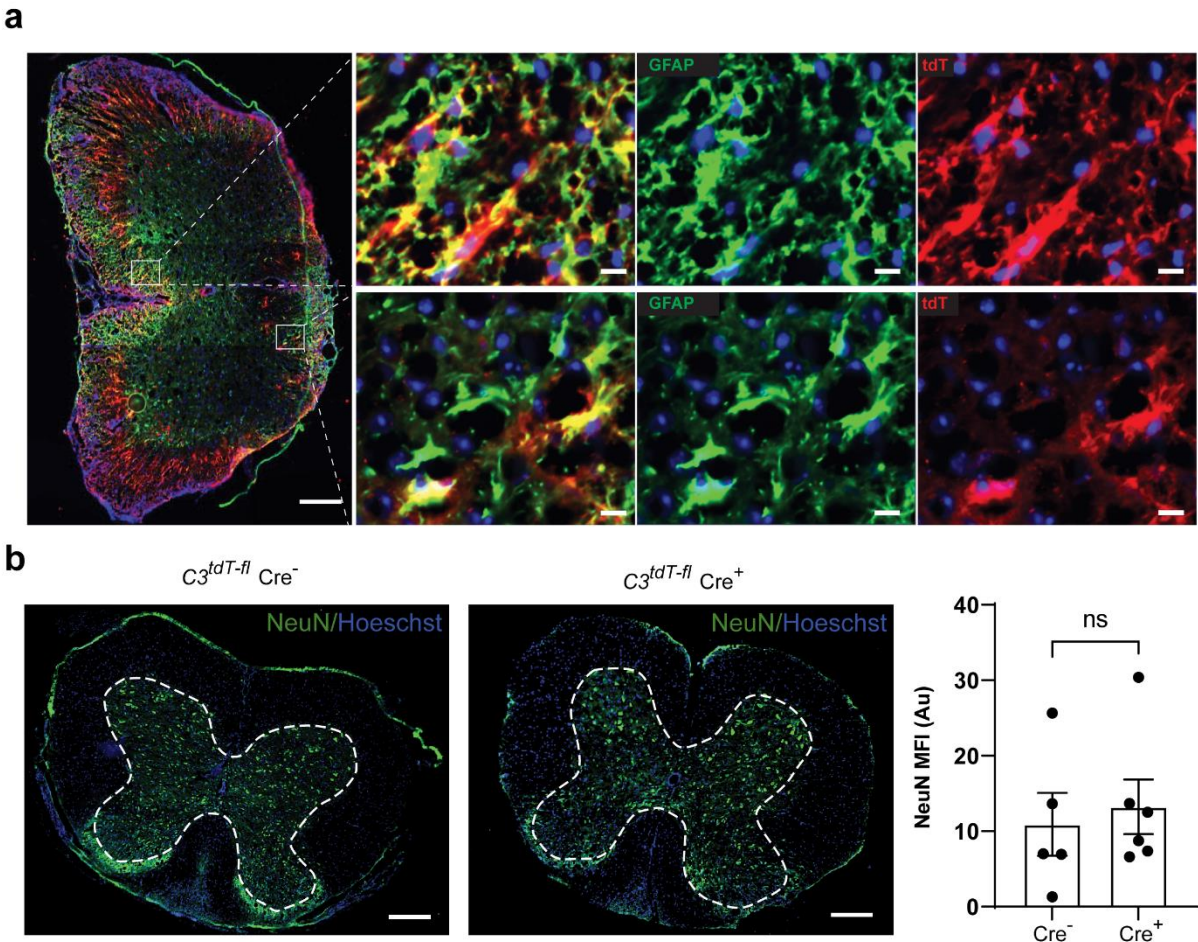
(a) Flow plots showing gating strategy for analyzing leukocytes in brain and spinal cord of peak EAE $C3^{+/+}$ and $C3^{-/-}$ mice. (b-c). Quantification of IFN γ (b) and IL-17a+ (c) CD4+ T-cells in the brains of peak EAE mice. (d-h). Quantification of CD4+ T-cells (d), IFN γ and IL-17a+ CD4+ T-cells (e-f), infiltrating myeloid (g) and microglia (h) in the spinal cord of peak EAE mice.

Comparisons were done using 2-sided student t test with significance defined as having $p < 0.05$.



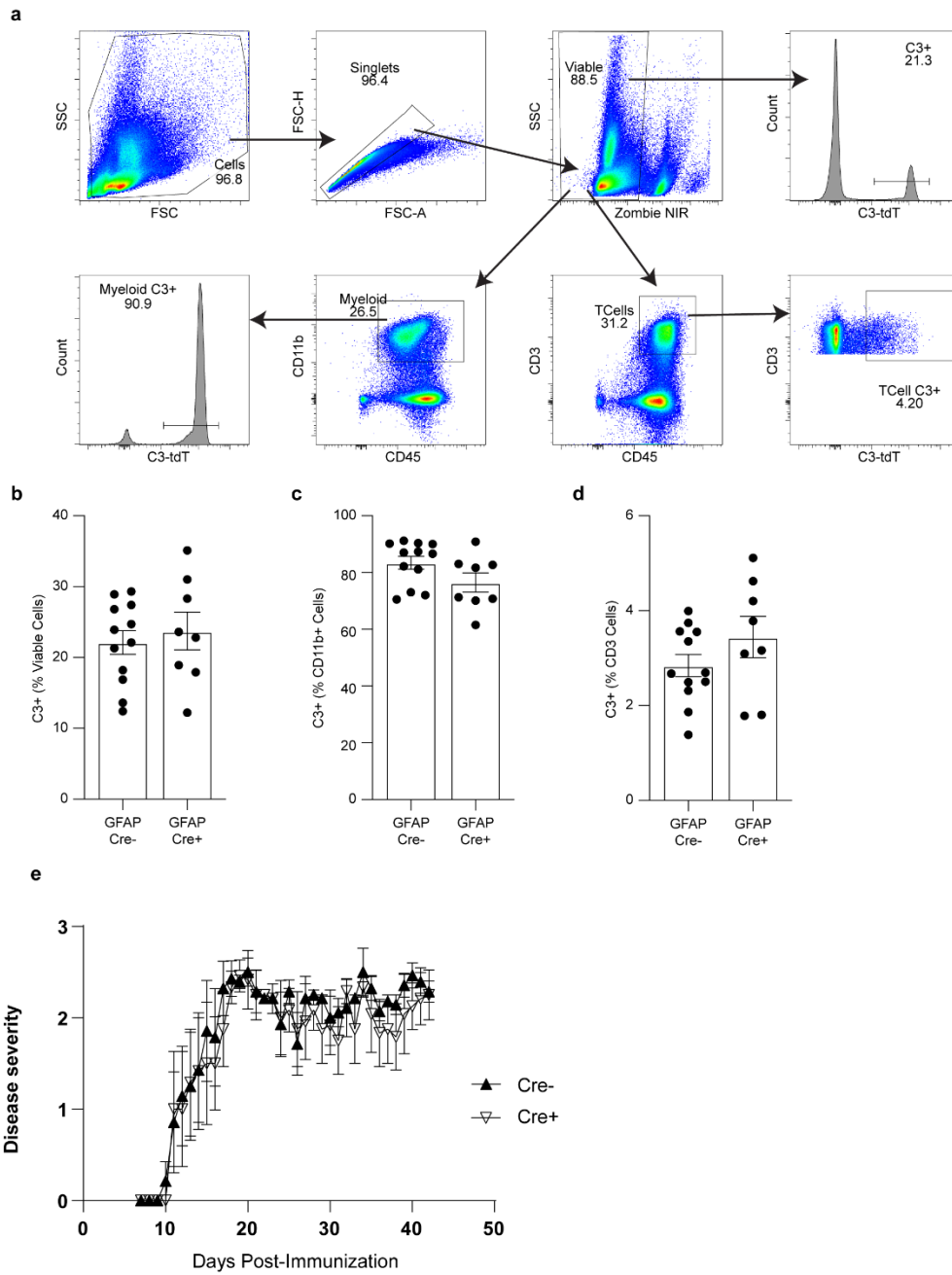
Supplementary Fig 4. C3 Depletion does not suppress EAE in a second independent strain.

EAE behaviors score of C57/BL6N $C3^{tdT-fl}$ mice crossed with a global Cre ($C3^{-/-}$) compared to the control group ($C3^{+/+}$). Error bar represents SEM.



Supplementary Fig 5. Astrocytes express C3 in the Spinal Cord of EAE mice without affecting Neuronal Mean Fluorescent Intensity.

Spinal cords from $C3^{tdT-fl}$ reporter mice were sectioned and stained for astrocyte and neuronal markers in addition to tdTomato. **(a)** Representative image of a spinal cord from a $C3^{tdT-fl}$ reporter mouse stained with GFAP (green), tdTomato (red), and nuclear stain DAPI. Scale bar =200 μ m. Magnified panels show extensive co-localization of GFAP with the C3 reporter tdTomato. Scale bars =10 μ m. **(b)** Representative images of spinal cords from $C3^{tdT-fl} \times GFAP-Cre^{-}$ and $C3^{tdT-fl} \times GFAP-Cre^{+}$ mice stained with NeuN (green) and nuclear stain Hoechst. Scale bar =500 μ m. Regions of interest were made encapsulating the central grey matter of each section (shown by the dashed white line), and the NeuN MFI was determined. Each data point represents one cervical section from one animal.



Supplementary Fig 6. GFAP-Cre does not alter peripheral C3 expression.

Spleens from EAE PID16 in $C3^{tdT-fl} \times GFAP-Cre^{-}$ and in $C3^{tdT-fl} \times GFAP-Cre^{+}$ mice were collected and C3 expression was assessed using flow cytometry. **(a)** Flow gating schematic of

splenocytes showing C3-tdT measurement in viable cells and in myeloid (CD11b⁺) and T-Cell (CD3⁺) populations. **(b-d)** Quantification of cells expressing C3 as a percent of viable cells **(b)**, myeloid cells **(c)**, and T-cells **(d)**. Each point represents an individual animal. Data is from two independent experiments. **(e)** EAE behavioral score of $C3^{tdT-fl}$ x GFAP Cre⁺ vs GFAP Cre⁻ mice. Error bar represents SEM.